Minor Genetic Consequences of a Major Mass Mortality: Short-Term Effects in *Pisaster ochraceus*

Lauren M. Schiebelhut[1,†,*], Melina Giakoumis[2,3,†], Rita Castilho[4,5], Paige J. Duffin[6], Jonathan B. Puritz[7], John P. Wares[6], Gary M. Wessel[8], and Michael N Dawson[1]

[1] Life and Environmental Sciences, University of California, Merced, 5200 N. Lake Road, Merced, California 95343
[2] Graduate Center, City University of New York, 365 5th Avenue, New York, New York 10016
[3] Department of Biology, City College of New York, 160 Convent Avenue, New York, New York 10031
[4] University of Algarve, Campus de Gambelas, Faro, Portugal
[5] Center of Marine Sciences (CCMAR), Campus de Gambelas, Faro, Portugal
[6] Odum School of Ecology and Department of Genetics, University of Georgia, 120 Green Street, Athens, Georgia 30602
[7] Department of Biological Sciences, University of Rhode Island, 120 Flagg Road, Kingston, Rhode Island 02881
[8] Department of Molecular Biology, Cell Biology, and Biochemistry, Brown University, Providence, Rhode Island 02912

Abstract

Mass mortality events are increasing globally in frequency and magnitude, largely as a result of human-induced change. The effects of these mass mortality events, in both the long and short term, are of imminent concern because of their ecosystem impacts. Genomic data can be used to reveal some of the population-level changes associated with mass mortality events. Here, we use reduced-representation sequencing to identify potential short-term genetic impacts of a mass mortality event associated with a sea star wasting outbreak. We tested for changes in the population for genetic differentiation, diversity, and effective population size between pre–sea star wasting and post–sea star wasting populations of Pisaster ochraceus*—a species that suffered high sea star wasting-associated mortality (75%–100% at 80% of sites). We detected no significant population-based genetic differentiation over the spatial scale sampled; however, the post–sea star wasting population tended toward more differentiation across sites than the pre–sea star wasting population. Genetic estimates of effective population size did not detectably change, consistent with theoretical expectations; however, rare alleles were lost. While we were unable to detect significant population-based genetic differentiation or changes in effective population size over this short time period, the genetic burden of this mass mortality event may be borne by future generations, unless widespread recruitment mitigates the population decline. Prior results from* P. ochraceus *indicated that natural selection played a role in altering allele frequencies following this mass mortality event. In addition to the role of selection found in a previous study on the genomic impacts of sea star wasting on* P. ochraceus*, our current study highlights the potential role the stochastic loss of many individuals plays in altering how genetic variation is structured across the landscape. Future genetic monitoring is needed to determine long-term genetic impacts in this long-lived species. Given the increased frequency of mass mortality events, it is important to implement demographic and genetic monitoring strategies that capture baselines and background dynamics to better contextualize species' responses to large perturbations.*

Received 28 August 2021; Accepted 16 August 2022; Published online 4 January 2023.
* Corresponding author: lschiebelhut@ucmerced.edu.
† Equal first authors.
Abbreviations: DAPC, discriminant analysis of principal components; MME, mass mortality event; SFS, site frequency spectra; sNMF, sparse non-negative matrix factorization; SNP, single-nucleotide polymorphism; SSW, sea star wasting.
Online enhancements: appendix, supplemental code.

The Biological Bulletin, December 2022, volume 243, number 3: 328–338. https://doi.org/10.1086/722284

Introduction

The magnitude and frequency of mass mortality events (MMEs) are increasing (Fey *et al.*, 2015). Largely due to anthropogenic change (IPBES, 2019; IPCC, 2021), chronic and acute environmental perturbations are more intense and include, but are not limited to, higher temperatures (Oliver *et al.*, 2018), lower ocean pH (Wootton *et al.*, 2008), expansion of hypoxic dead zones (Altieri and Kiaz, 2019), and harmful algal blooms (HABs) (McCabe *et al.*, 2016). Individual events can have profound impacts on populations, illustrated by mass mortality in multiple species following an HAB (Jurgens *et al.*, 2015), in kelp following a heat wave (Gurgel *et al.*, 2020), and in Dungeness crab following hypoxia (Chan *et al.*, 2019). The intervals between such extreme perturbations also are becoming shorter, interrupting recoveries that may require a decade or more (Fabina *et al.*, 2015; Vercelloni *et al.*, 2020). This compounds stressful impacts of these events and leaves populations more vulnerable to subsequent assaults (Dietzel *et al.*, 2020). In the Great Barrier Reef, coral recovery rates have declined by 84% between 1992 and 2010 in correlation with chronic stressors and repeated acute disturbances in the region (Ortiz *et al.*, 2018). Increasingly, multiple environmental assaults are superimposed (*e.g.*, McPherson *et al.*, 2021). In the near future, marine systems are predicted to experience mass extinctions on par with other great extinctions throughout Earth's history as a result of anthropogenic climate change (Penn and Deutsch, 2022).

The consequences of past MMEs have been devastating, clearly illustrated by changes in censused populations. For example, surveys of the pen shell (*Pinna nobilis*), bull kelp (*Nereocystis luetkeana*), and common murre (*Uria aalge*) have shown precipitous population declines (Vázquez-Luis *et al.*, 2017; Rogers-Bennett and Catton, 2019; Piatt *et al.*, 2020). Such large decreases in census population size are expected to impact genetic diversity and effective population size (N_e). At reduced population sizes, rare alleles may be lost through genetic drift and limited reproduction due to low densities of reproductive individuals; these consequences further lead to reduced genetic mixing and loss of diversity (Pujolar *et al.*, 2011). In two kelp forest-forming species, a recent marine heat wave led to losses of ~30%–65% of the genetic diversity, in some cases leaving only a single dominant haplotype (Gurgel *et al.*, 2020). Understanding the prevalence and magnitudes of losses of intraspecific diversity is increasingly important as global anthropogenic change threatens biodiversity. Standing genetic variation provides the source material on which selection can act during changing conditions, so losing rare diversity could limit the flexibility of populations to respond to future stressors (Radwan *et al.*, 2010; Du *et al.* , 2016). Previous work on MMEs has provided evidence of selection for advantageous alleles (*e.g.*, Lessios, 1988; Pilczynska *et al.*, 2016; Campbell-Staton *et al.*, 2017; Padrón *et al.*, 2018; Schiebelhut *et al.*, 2018)—an important process that can help promote recovery. Exploring intraspecific population genomic patterns in the short term may therefore help reveal the genetic consequences of MMEs in the long term.

Species for which changes in genetic diversity can be assessed following an MME are rare because they require that a baseline genetic assessment was collected before the perturbation event. Often, we are left with only the aftermath and no record of what was lost. The ochre sea star, *Pisaster ochraceus*, is one of a small, but growing, number of exceptions. *Pisaster ochraceus* is distributed across the western coastline of North America from south-central Alaska to southern Baja California, Mexico (Lambert, 2000), has pelagic planktotrophic larvae, and is an ecologically important keystone predator in the rocky intertidal (Paine, 1966). This species suffered major mortality (75%–100% mortality at 80% of sites) across its geographic range during the sea star wasting (SSW) outbreak that began in 2013 (Miner *et al.*, 2018), an outbreak that affected about 20 asteroid species (Hewson *et al.*, 2014) and the cause of which is still considered unresolved. Schiebelhut *et al.* (2018) found parallel signals of selection coinciding with the SSW outbreak across many geographic locations in north-central California. Here, using samples collected before and after the SSW event from a broader set of geographic locations (Fig. 1), we expanded on previous work by testing for the short-term effects of mass mortality on diversity, population genetic differentiation, and genetic estimates of N_e in *P. ochraceus*. Because genetic samples were collected across a broad geographic area and preserved prior to the recent major mortality event, this SSW-affected system provided a rare opportunity to evaluate the short-term genetic impacts of mass mortality on an ecologically important species.

Materials and Methods

Sample collection, DNA extraction, and sequencing

To explore population genetic patterns in *Pisaster ochraceus* (Brandt, 1835) before (pre-SSW) and after (post-SSW) major SSW-associated mortality, we subsampled tube feet from specimens used in Harley *et al.* (2006) and made new collections following major mortality. For pre-SSW *versus* post-SSW comparisons, we sampled 7 to 10 intertidal individuals from each of 8 locations from Washington, Oregon, and California from 2003 to 2005 (Harley *et al.*, 2006) (n = 72)—well before the major wasting outbreak began in 2013—and from complementary locations during the SSW outbreak in 2013–2015 (n = 72) (Fig. 1; Table S1, available online), after major mortality was documented (Miner *et al.*, 2018). Additional sites were sampled in 2013–2015 to estimate the broadscale population genetic differentiation in adult *P. ochraceus* and available new recruits (Table S2, available online). We extracted DNA from tube feet that were preserved in 95% ethanol or dimethyl sulfoxide (DMSO)-enriched buffer, using a silica-based filter plate (5053; Pall, Slow Low, AZ) (Ivanova *et al.*, 2006). For each specimen,

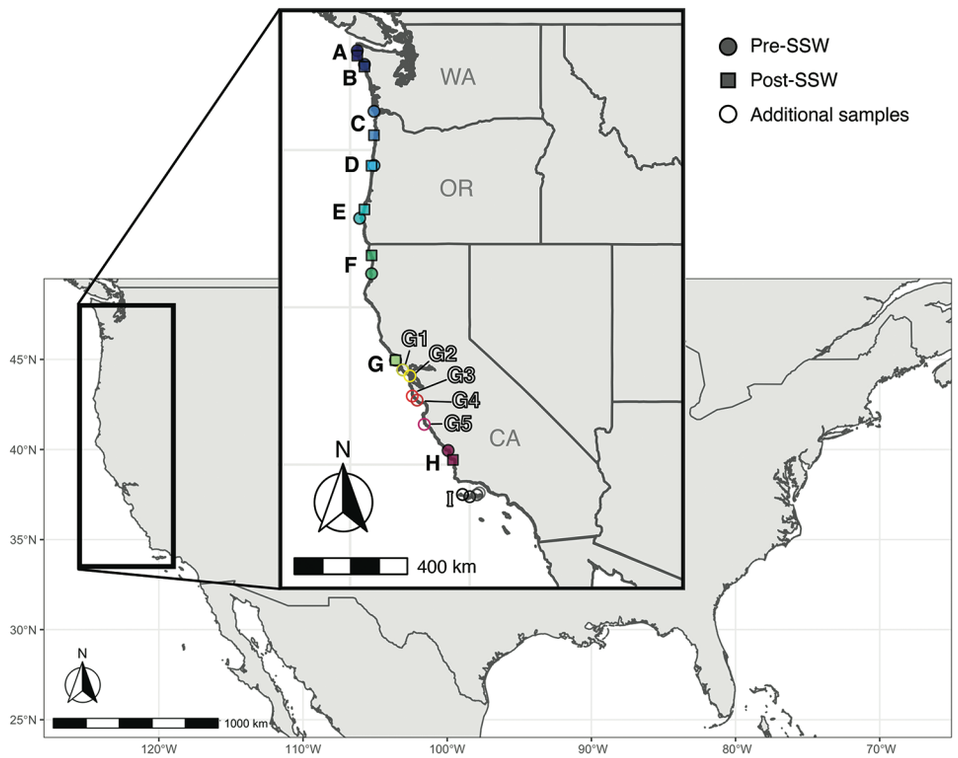

Figure 1. Sampling locations for *Pisaster ochraceus* collected before (shaded squares) and after (shaded circles) the 2013 wasting outbreak in locations A–H, which are distributed from northern Washington through southern California. These samples were used to ensure a balanced study design for comparisons of pre- and post-sea star wasting (SSW) populations. Open circles represent sites for which additional individuals were sampled for estimates of contemporary population genetic structure (locations A–H plus G#–I).

50–100 ng μL^{-1} of DNA in 25 μL of 10 mmol L^{-1} Tris HCl was submitted to the Genomic Sequencing and Analysis Facility (GSAF) at the University of Texas at Austin for quantitation, normalization, double digestion with the EcoRI and MspI restriction enzymes (Peterson *et al.*, 2012), size selection for 300 ± 50 bp using custom bead preparation (GSAF), adaptor ligation, purification, and 2 × 150 paired-end sequencing on an Illumina HiSeq 4000 (San Diego, CA).

Sequence processing

We demultiplexed sequences by using process_radtags from Stacks v.1.35 (Catchen *et al.*, 2011), allowing a maximum of two mismatches in the barcode and deposited raw sequences in the Sequence Read Archive (SRA) of the National Center for Biotechnology Information (NCBI) under BioProject PRJNA871810 or previously under accession numbers SRS3098330–SRS3098334, SRS3098336, and SRS3098439. We used dDocent v.2.2.13 (Puritz *et al.*, 2014) with default parameters to trim low-quality bases (*i.e.*, with a quality score <20 and using a sliding 5-bp window if average quality dropped <10), map paired-end reads (*i.e.*, using the MEM algorithm of Burrows-Wheeler Aligner with a match score of 1, a mismatch score of 3, and a gap opening penalty of 5), and call single nucleotide polymorphisms (SNPs) (*i.e.*, using FreeBayes [Garrison and Marth, 2012] with a minimum mapping and base quality score of PHRED 10). Trimmed reads were directly mapped to the *P. ochraceus* genome (NCBI BioProject PRJNA532896, SUB5448653; Ruiz-Ramos *et al.*, 2020). We filtered genotyped SNPs (see commented code, available online), using VCFtools v.0.1.15 (Danecek *et al.*, 2011) and custom scripts (Puritz *et al.*, 2016; Puritz, 2022)—following the same approach used in Schiebelhut *et al.* (2018). Three different SNP sets were generated for various analyses (Fig. S1, available online) to accommodate our study design and best practices for each analysis type. Set 1 included individuals used in the pre- *versus* post-SSW comparison (Table S1, available online); the final filtered vcf file had a 98% genotype call rate across all individuals (with maximum allowed missing loci per individual of 13%), minimum depth of 20 (maximum of 164; yielding mean of 106) per SNP, and minor allele frequency (MAF) of at least 0.01. To control for linkage disequilibrium, we retained one SNP per RAD (restriction site-associated DNA) locus by applying the –thin 500 option in VCFtools. Processing for SNP set 2 differed from set 1 in that we did not thin SNPs or apply the MAF filter (*i.e.*, singleton SNPs were allowed); this modification is necessary to detect changes in rare alleles in (SFS)-based analyses. Set 3 included additional individuals and geographic locations from the post-SSW population but otherwise underwent the same sample processing as set 1 (Fig. S1). The SNP sets were used for different analyses based on program recommendations and study design.

Population genetic analyses

We used the genetic data to explore primary signatures and spatial patterns of genome-wide diversity within each time period and contrasting the pre-SSW and post-SSW outbreak populations of *P. ochraceus*. First, we evaluated range-wide population genomic structure that may drive the anecdotally distinct responses in different portions of the coast (Menge *et al.*, 2016). We used sparse non-negative matrix factorization (sNMF) (Frichot *et al.*, 2014) to assess population structure separately in pre-SSW and post-SSW *P. ochraceus* populations, using SNP set 1. The sNMF method models each individual's ancestry coefficients and selects the most likely number of ancestral gene pools (K), using a cross-entropy criterion that searches for minimal error when a subset of hidden genotypes are re-predicted by the inferred ancestry coefficients. To further evaluate population genetic structure, we calculated global F_{ST} and 95% confidence intervals (CIs), using the Weir and Cockerham (1984) method in diveRsity v.1.9.90 (Keenan *et al.*, 2013) in R for populations sampled before and after major mortality separately. We also conducted a principal component analysis (PCA), using glPca in adegenet v.2.0.2 (Jombart and Ahmed, 2011) in R (R Core Team, 2020), adding in the broader set of contemporary *P. ochraceus* samples (Table S2, available online), using SNP set 3 (Fig. S1, available online).

To further explore axes of variation in post- relative to pre-SSW populations, we conducted a discriminant analysis of principal components (DAPC)—defining 3 geographic regions (ABC, DE, and FGH, comprised of our 8 locations; Fig. 1) and 2 time points (pre-SSW and post-SSW) *a priori*—retaining 24 PCs and 5 discriminant functions (n groups − 1) in adegenet v.2.0.2 (Jombart and Ahmed, 2011) in R using SNP set 1. Because pre-SSW and post-SSW sampling sites were similar but not identical, regional clustering (*i.e.*, ABC, DE, and FGH) allowed us to investigate regional differences without pairing non-identical sites between time points; this enabled us to detect any localized differences while still maintaining a balanced number of samples across regions. Finally, to explore how variation was partitioned at each time point, we conducted an analysis of molecular variance (AMOVA) for the two time points separately, with nested structure by site and region. We evaluated significance after correcting for multiple testing (Benjamini and Hochberg, 1995) using a randomization test with 999 permutations in the R package ade4 (Dray and Dufour, 2007).

To further evaluate potential differences between these groups and the short-term genomic consequences of SSW, we calculated expected and observed heterozygosity using hierfstat v0.5-7 (Goudet, 2005) in R and Tajima's D, Fu and Li's D^*, and Fu and Li's F^* using DnaSP v6.12.03 (Rozas *et al.*, 2017) (using SNP set 1 and 2) for the pre-SSW and post-SSW populations separately. As a complement to these tests, and to evaluate the potential loss of rare alleles, we calculated the general SFS for each time point in easySFS (Overcast, 2022), using SNP set 2, and applied a projection method that corrects for missing data in RADseq datasets (as in Marth *et al.*, 2004) with a chosen projection value that maximized segregating sites in the SNP data (Gutenkunst *et al.*, 2009). We visualized the SFS by displaying the number of SNPs that occur at each frequency, up to 40 (*i.e.*, singletons, doubletons, *etc.*). We used these statistics to detect indicators of demographic and selection-driven changes in diversity.

Finally, using SNP set 1, we estimated N_e by using the linkage disequilibrium (Hill, 1981; Waples, 2006; Waples and Do, 2010) test, as implemented in NeEstimator (Do *et al.*, 2014), for pre- and post-SSW individuals separately and calculated parametric and jackknife 95% CIs. This approach complemented our inferences of what types of diversity were lost during the mass mortality of SSW and allowed us to contextualize these data with overall population census size estimates and consider arguments that have been made about periodic cyclic demography in asteroids (Uthicke *et al.*, 2009).

Results

The three separate filtered datasets we used to explore short-term genetic impacts of mass mortality yielded 1040 SNPs for set 1, 12,020 SNPs for set 2, and 2902 SNPs for set 3 (Fig. S1, available online). The sNMF analysis on SNP set 1 indicated that *P. ochraceus* has only one genetic group ($K = 1$) both before and after mortality (Fig. S2, available online). Likewise, estimates of global F_{ST} confirm the absence of significant population genetic structure for both pre-wasting ($F_{ST} = 0.0001$; 95% CI: −0.0161 to 0.0214) and post-wasting ($F_{ST} = 0.0021$; 95% CI: −0.0140 to 0.0206) populations. The PCA, using the expanded set of samples (Table S2, available online; SNP set 3), did not reveal any clustering by geographic location, timing of sampling, or adult *versus* recruit status (Fig. S3, available online). The slight clustering that is seen on PC axis 1 seems likely to be driven by paralogs or copy number variants in the random subset of high-loading SNPs we visualized in the alignment.

We used DAPC on SNP set 1 to further evaluate the spatial distribution of genetic variation. This clustering method revealed two relevant axes of variation, with the first discriminant function (DF1) distinguishing geography and the second discriminant function distinguishing post-SSW from pre-SSW, though with substantial amounts of overlap (Fig. 2A). Centroids of the three pre-SSW regions were more closely clustered on DF1 than the centroids of post-SSW regions (Fig. 2A). We confirmed that this pattern was not driven by excessive observed heterozygosity (relative to expected heterozygosity; Fig. S4, available online); the SNPs with the highest loadings in the DAPC did not overlap with the SNPs with heterozygosities >0.75 in Figure S4. The AMOVA revealed that the vast majority of

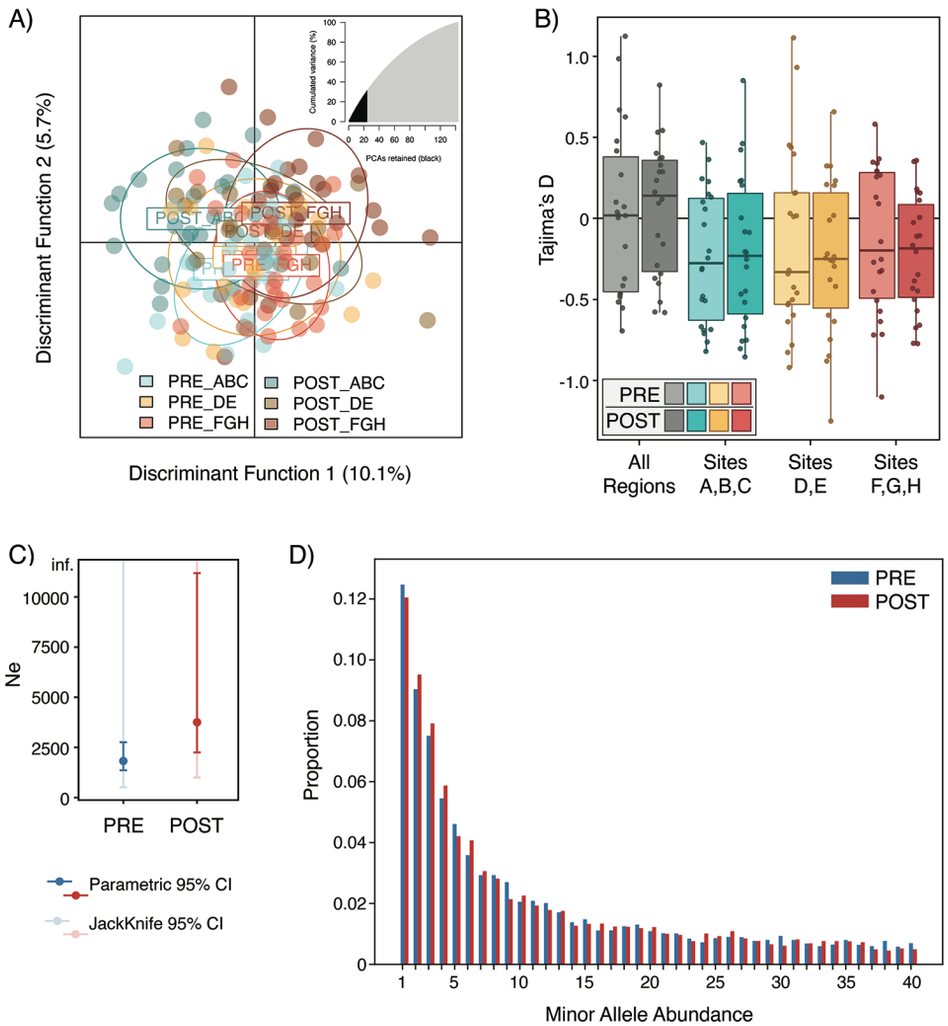

Figure 2. Genetic analysis of *Pisaster ochraceus* sampled before mass mortality (2003–2005) and after mass mortality (2014–2015) associated with sea star wasting (SSW). (A) Discriminant analysis of principal components (retaining 24 principal components) with coastal regions (ABC, DE, and FGH, which correspond to groups of clustered sampling locations) and time points (pre- and post-SSW) defined *a priori*. (B) Tajima's *D*; each data point represents the mean for each of the 22 chromosomes in *P. ochraceus*. For the box-and-whisker plots, the box corresponds to the median and first and third quartiles, and the whiskers correspond to 1.5 × IQR (interquartile range); points outside the whisker range represent outliers. (C) Effective population size calculated using the linkage disequilibrium method across all samples; error bars represent 95% confidence intervals (dark: parametric; light: jackknife). (D) Site frequency spectra for pre- and post-wasting populations summarizing the number of single-nucleotide polymorphisms that occur at each frequency for each time point.

the variance (>99%) originates from within individual sampling locations, both pre- and post-SSW (Table S3, available online). A small portion of the variance originated from between sites within regions (pre: 0.11%; post: 0.66%), with the post-SSW population trending toward greater structure than predicted by chance ($P = 0.051$ after adjustment for multiple tests); additional genetic metrics also revealed similarities and differences between the separately tested time points. Mean observed heterozygosity had minimal change from pre-SSW ($H_o = 0.1846$) to post-SSW ($H_o = 0.1819$), with a similar pattern of observed *versus* expected heterozygosity at both time points (Fig. S4). Tajima's *D* was not different from zero for pre-wasting (0.03; 95% CI: −0.18 to 0.24) or post-wasting (0.05; 95% CI: −0.11 to 0.21). Post-wasting Tajima's *D* did not differ from pre-wasting, overall or by sub-region, but trended toward being slightly higher in the post-wasting population (Fig. 2B). Fu and Li's D^* and Fu and Li's F^* showed similar overall patterns but variable sub-regional patterns (Fig. S5, available online), with Fu and Li's D^* increasing from 1.0 pre-wasting (95% CI: 0.82–1.18) to 1.49 post-wasting (95% CI: 1.31–1.65) and Fu and Li's F^* increasing from 0.72 pre-wasting (95% CI: 0.57–0.88) to 1.04 post-wasting (95% CI: 0.87–1.21). However, when singletons were included in the analysis, this difference was attenuated, although the relative difference between pre- and post-SSW for these two statistics remained (Fig. S6, available online). The SFS analysis of SNP set 2 revealed a loss of rare singletons from 12.67% of variant sites

pre-SSW to 12.05% of variant sites post-SSW. We also detected an increase in the proportion of doubletons, from 9.03% of variant sites to 9.50%, which means that the ratio of singleton to doubleton shifted from 0.713 to 0.790 from pre- to post-SSW, as shown by changes in the visualized SFS (Fig. 2D).

Estimates of N_e did not decrease following mass mortality. The pre-SSW genetic estimate of N_e was 1,511 (95% CI: parametric 1360–2761, jackknife 510–inf.), and the post-SSW estimate was 2491 (95% CI: parametric 2251–11,191, jackknife 1000–inf.), with wide and overlapping CIs (Fig. 2C).

Discussion

Pisaster ochraceus is the most completely studied sea star species in the context of the contemporary SSW event, including both pre-outbreak and post-outbreak populations (*e.g.*, Miner *et al.*, 2018; Schiebelhut *et al.*, 2018). According to our analyses, *P. ochraceus* lacks overall population genetic differentiation and, given that the responses of genomic diversity are comparable across the subregions defined in this paper—regardless of perceived spatial variance in response, for example, to aspects of environmental variation (Eisenlord *et al.*, 2016; Menge *et al.*, 2016)—there was an overall loss of rare diversity (Fig. 2). This is as would be expected in a strong bottleneck (Nei, 1987), albeit small, and a similarly slight shift toward more genetic differentiation between locations following mass mortality.

Pisaster ochraceus suffered mass mortality across its geographic range (75%–100% mortality at 80% of sites) (Miner *et al.*, 2018); but a concomitant decline was not detected in estimates of N_e (Fig. 2C), consistent with population genetic theory. Although small sample sizes can limit our ability to accurately estimate N_e, which likely leads to underestimates (Waples, 2005, 2006, 2016; Waples and Do, 2010), N_e estimates using the linkage disequilibrium (LD) method tended to stabilize when at least 1500 SNPs are used (Marandel *et al.*, 2020)—a number we closely approached after accounting for potential linkage. Furthermore, because our approach was designed to evaluate whether a very recent massive demographic decline might change the estimate of contemporary N_e relative to pre-SSW N_e (as opposed to estimating an absolute N_e value), we still should be able to identify a detectable signal representing the shift between pre- and post-SSW-associated mass mortality using the LD method if that signal is indeed present in the data. The fact that we do not detect a change in N_e following mass mortality is, however, explainable by the observation that genomic signatures of a decline in N_e may lag, whereby accurate detection is thought to be possible only after 3–10 generations after the initial decline (Keller *et al.*, 2001; Nunziata and Weisrock, 2017). If we assume that generation time for *P. ochraceus* is comparable to that of another sea star species with similar life-history traits, *Pycnopodia helianthoides* (whose conservative age range is estimated at ~27–37 years; Gravem *et al.*, 2021), then only ~0.31 generations have elapsed between sampling time points and, importantly, effectively zero have elapsed since the MME. Even with more rigorous sampling of the *P. ochraceus* genome data from multiple time points, we may never see a strong signal of the large 2013–2015 census population decline reflected in associated genetic estimates of N_e because of a widespread recruitment event that occurred during the same time period. In some regions throughout the species' range, documented recruitment was many times greater than was seen in previous years (Menge *et al.*, 2016; Miner *et al.*, 2018). Another species, the sunflower star (*Pycnopodia helianthoides*), was not as fortunate, suffering even greater magnitudes of decline and no signs of rebound through much of its range (Gravem *et al.*, 2021); this species may tell a different story.

Our estimates of N_e for both pre- and post-SSW (Fig. 2C) may seem low for a marine species with very large population sizes. However, these values are not unexpected for populations that cyclically contract and recover in boom-bust cycles, a common demographic feature in echinoderms (Uthicke *et al.*, 2009). Although we have exceedingly few estimates of N_e in asteroids for comparison (and none available that were estimated using genome-wide data), ancestral N_e and contemporary N_e have been estimated to be of similar scales in other asteroid species using coalescence-based methods (Puritz *et al.*, 2012, 2017). Marine diversity in general has been revealed to have low N_e/N ratios (Turner *et al.*, 2002).

Among the methods used to uncover genetic signatures of demographic change, heterozygosity is often considered a weak indicator of recent change (Nei, 1987; Wares *et al.*, 2005). Measured signals of decline in genetic diversity or loss of rare alleles can be detected before other signatures of a bottleneck event, such as declines in heterozygosity (Vilas *et al.*, 2015). For *P. ochraceus*, we found signatures of the MME as indicated by both a loss of rare alleles and a trend toward greater population differentiation in the post-SSW population relative to the well-mixed pre-SSW population (Fig. 1A; Table S3, available online).

Given our lack of definitive signal in this short time since the MME, this study emphasizes the crucial need for ongoing genetic monitoring. Tracking the next three to five generations will be especially important for *P. ochraceus*, as well as other asteroid species affected by the 2013 outbreak of SSW, to determine whether there are lasting genetic consequences of the sharp demographic decline and whether recruitment-led rebounds proceed quickly enough to avoid significant long-term impacts. Indeed, long-term monitoring of the species complex in the lecithotrophic brooding sea star *Leptasterias*, albeit retrospectively using museum specimens, illustrates changes in the distribution of genomic diversity across its range through time (Melroy and Cohen, 2021). Even so, the temporal and genetic resolution (*i.e.*, our ability to determine actual change) is limited, given

the high variance observed in these datasets. Mass mortality events (unrelated to SSW) were noted in *Leptasterias* in 2011 (Jurgens *et al.*, 2015), shortly followed by subsequent and significant losses due to SSW (Jaffe *et al.*, 2019). Variation in population size estimates and mitochondrial haplotypes in *Leptasterias* observed at different locations along the west coast of the United States, however, suggest more demographic turnover—or shifting of the relative proportions of individuals from a particular genetic background in the population—than would be expected for brooding star species, which are generally thought to have higher levels of population structure due to their low dispersal abilities (Melroy *et al.*, 2017; Melroy and Cohen, 2021). By contrast, planktotrophic sea stars, such as *P. ochraceus* evaluated here, are expected to demonstrate high cyclic demographic changes due to an increased dispersal capacity and opportunity for admixture (Uthicke *et al.*, 2009). However, there are very few examples in the literature demonstrating how genetic variation, and its spatial distribution, change through time (Fenderson *et al.*, 2020). Therefore, the predicted genomic dynamics and their relationships to life-history traits remain to be studied and clarified in more detail.

In the case of *P. ochraceus*, we find little evidence of dramatic change in genetic diversity and—despite a small trend toward greater differentiation between sites in the post-SSW population—the absence of strong signatures of any shifts that describe how that diversity is distributed by age or frequency. Nakamura *et al.* (2018) note that organisms with periodicity in census size only generate strong signatures in tests such as Tajima's *D* when the periodicity is long relative to the N_e. Our estimates of Tajima's *D* trended toward being more positive in the post-SSW population relative to pre-SSW, indicating a reduction in rare alleles; however, the 95% CIs spanned zero and included the mean of each time point (Fig. 2B). The trending increase in Fu and Li's D^* and F^* to more positive values in post-SSW relative to pre-SSW (Figs. S5, S6, available online) indicates a shift to fewer unique variants, suggesting that common variants became more common.

Our study design, comparing recent historical to recent post-mortality populations, provides an intriguing reference point for interpretation. Though our dataset provides a rare opportunity to study the immediate effects of an MME, we reserve interpretation of whether it is a harbinger for long-term population effects of SSW on *P. ochraceus*, given that we captured and characterized survivors of the event and not subsequent generations. Additionally, though natural selection has occurred and is quite strong in *P. ochraceus* (Schiebelhut *et al.*, 2018), the majority of SNPs generated using reduced-representation sequencing (ddRAD) evaluated to date have captured only a small portion (~3%) of the genome (Ruiz-Ramos *et al.*, 2020). Broader sequencing approaches, such as whole-genome resequencing, could help resolve some of our uncertainty and are needed to capture a larger portion of the genomic response. That said, processes driven by genetic drift, such as a reduction in genomic diversity and/or N_e, affect the entire genome and should be evident in any random sample of loci.

An important consideration when trying to detect genomic signatures of MMEs in marine populations is the tendency of broadcast-spawning marine invertebrates to have high levels of both contemporary and ancestral genetic polymorphisms. *Pisaster ochraceus* has previously been shown to have moderate to high levels of genetic polymorphisms (Harley *et al.*, 2006; Schiebelhut *et al.*, 2018); likewise, other broadcast-spawning asteroid species along the west coast of North America have proven to be incredibly diverse (Keever *et al.*, 2009; Puritz and Toonen, 2011), with inferred ancestral population sizes in the hundreds of thousands or more (Hart and Marko, 2010; McGovern *et al.*, 2010). Single-sample estimates of N_e, even those that include large numbers of loci, can be problematic when N_e is large (Hare *et al.*, 2011); these scenarios typically require intensive sampling of individuals (Ovenden *et al.*, 2007; Palstra and Ruzzante, 2008; Waples and Do, 2010). Similar concerns of power and sample size apply to estimates of genetic structure in highly polymorphic species with high gene flow (Ryman *et al.*, 2006; Morin *et al.*, 2009; Haasl and Payseur, 2011; Flesch *et al.*, 2018), which also describes *P. ochraceus* and many other sea stars.

Nonetheless, the declines in abundance seen across many asteroid species in the northeastern Pacific due to SSW (M. N Dawson et al., unpubl. data; L. M. Schiebelhut et al., unpubl. data) threaten loss of intraspecific genetic variation that is often crucial to the resilience and health of ecosystems (Des Roches *et al.*, 2021). Thus, it is important to develop genetic monitoring of wild populations that can identify genetic declines before widespread loss, especially given that MMEs are increasing in frequency and magnitude. Over time, the compounding effect of repeated stressors could change patterns of decline and recovery. An essential component of any such monitoring program will be to establish baselines; without such baselines, it is impossible to determine what is being lost and what can be done to mitigate the decline of particular populations and erosion of diversity. Taking the genetic pulse of populations, including capturing gene expression, may allow early detection of stressors that may otherwise go unnoticed until a substantial decline is seen in census population size. Population genomic analysis of contemporary time series data creates an unique opportunity to assess genomic responses to MMEs against normal background fluctuations in allele frequencies—for which we know very little for most asteroid species. In addition, while much of the research and management focus has been on rare (although increasingly frequent; Fey *et al.*, 2015) large mass mortalities, genetic monitoring would also foster a better understanding of background mortality (*e.g.*, following seasonal changes, post-settlement, or other intermittent events, such as harmful algal blooms, hypoxia, storms, *etc.*) and help identify the

relative impacts of drift, migration, and selection (Gompert *et al.*, 2021).

Acknowledgments

The virtual workshop supporting development of this project and participation of and data from JPW, MND, LMS, and PJD were funded by National Science Foundation (NSF) grants OCE-1737091 and OCE-1737381. Participation of RC in the virtual workshop was funded by Portuguese national funds from Foundation for Science and Technology (FCT) through project UIDB/04326/2020. *Pisaster ochraceus* collections in 2014–2015 and sequencing were supported by a National Park Service award to Peter Raimondi (MCA A00-1228-S002). Study design: LMS, MG, MND, JBP, JPW. Execution of research and analyses: LMS, MG. Manuscript preparation: LMS, MG, MND, RC, PJD, JBP, JPW, GMW. All authors approve this version and accept accountability for the authenticity of the study.

Data Accessibility

The sequences reported in this paper have been deposited in the National Center for Biotechnology Information sequence read archive under BioProject PRJNA871810 or previously under accession numbers SRS3098330–SRS3098334, SRS3098336, and SRS3098439. Filtered VCF files with single-nucleotide polymorphisms as well as specimen lists used in analyses are deposited in Dryad (https://doi.org/10.6071/M3R08X).

Literature Cited

Altieri, A. H., and R. J. Diaz. 2019. Dead zones: oxygen depletion in coastal ecosystems. Pp. 453–473 in C. Sheppard, ed. *World Seas: An Environmental Evaluation*. Academic Press, London.

Benjamini, Y., and Y. Hochberg. 1995. Controlling the false discovery rate: a practical and powerful approach to multiple testing. *J. R. Stat. Soc. B Stat. Methodol.* **57:** 289–300.

Campbell-Staton, S. C., Z. A. Cheviron, N. Rochette, J. Catchen, J. B. Losos, and S. V. Edwards. 2017. Winter storms drive rapid phenotypic, regulatory, and genomic shifts in the green anole lizard. *Science* **357:** 495–498.

Catchen, J. M., A. Amores, P. Hohenlohe, W. Cresko, and J. H. Postlethwait. 2011. Stacks: building and genotyping loci *de novo* from short-read sequences. *G3* **1:** 171–182.

Chan, F., J. A. Barth, K. J. Kroeker, J. Lubchenco, and B. A. Menge. 2019. The dynamics and impact of ocean acidification and hypoxia. *Oceanography* **32:** 62–71.

Danecek, P., A. Auton, G. Abecasis, C. A. Albers, E. Banks, M. A. DePristo, R. E. Handsaker, G. Lunter, G. T. Marth, S. T. Sherry *et al.* 2011. The variant call format and VCFtools. *Bioinformatics* **27:** 2156–2158.

Des Roches, S., L. H. Pendleton, B. Shapiro, and E. P. Palkovacs. 2021. Conserving intraspecific variation for nature's contributions to people. *Nat. Ecol. Evol.* **5:** 574–582.

Dietzel, A., M. Bode, S. R. Connolly, and T. P. Hughes. 2020. Long-term shifts in the colony size structure of coral populations along the Great Barrier Reef. *Proc. R. Soc. B Biol. Sci.* **287:** 20201432.

Do, C., R. S. Waples, D. Peel, G. M. Macbeth, B. J. Tillett, and J. R. Ovenden. 2014. NeEstimator v2: re-implementation of software for the estimation of contemporary effective population size (N_e) from genetic data. *Mol. Ecol. Resour.* **14:** 209–214.

Dray, S., and A. B. Dufour. 2007. The ade4 package: implementing the duality diagram for ecologists. *J. Stat. Softw.* **22:** 1–20.

Du, L., C. Cai, S. Wu, F. Zhang, S. Hou, and W. Guo. 2016. Evaluation and exploration of favorable QTL alleles for salt stress related traits in cotton cultivars (*G. hirsutum* L.). *PLoS One* **11:** e0151076.

Eisenlord, M. E., M. L. Groner, R. M. Yoshioka, J. Elliott, J. Maynard, S. Fradkin, M. Turner, K. Pyne, N. Rivlin, R. van Hooidonk *et al.* 2016. Ochre star mortality during the 2014 wasting disease epizootic: role of population size structure and temperature. *Philos. Trans. R. Soc. B Biol. Sci.* **371:** 20150212.

Fabina, N. S., M. L. Baskett, and K. Gross. 2015. The differential effects of increasing frequency and magnitude of extreme events on coral populations. *Ecol. Appl.* **25:** 1534–1545.

Fenderson, L. E., A. I. Kovach, and B. Llamas. 2020. Spatiotemporal landscape genetics: investigating ecology and evolution through space and time. *Mol. Ecol.* **29:** 218–246.

Fey, S. B., A. M. Siepielski, S. Nusslé, K. Cervantes-Yoshida, J. L. Hwan, E. R. Huber, M. J. Fey, A. Catenazzi, and S. M. Carlson. 2015. Recent shifts in the occurrence, cause, and magnitude of animal mass mortality events. *Proc. Natl. Acad. Sci. USA* **112:** 1083–1088.

Flesch, E. P., J. J. Rotella, J. M. Thomson, T. A. Graves, and R. A. Garrott. 2018. Evaluating sample size to estimate genetic management metrics in the genomics era. *Mol. Ecol. Resour.* **18:** 1077–1091.

Frichot, E., F. Mathieu, T. Trouillon, G. Bouchard, and O. François. 2014. Fast and efficient estimation of individual ancestry coefficients. *Genetics* **196:** 973–983.

Garrison, E., and G. Marth. 2012. Haplotype-based variant detection from short-read sequencing. arXiv: 1207.3907 [q-bio.GN].

Gompert, Z., A. Springer, M. Brady, S. Chaturvedi, and L. K. Lucas. 2021. Genomic time-series data

show that gene flow maintains high genetic diversity despite substantial genetic drift in a butterfly species. *Mol. Ecol.* **30:** 4991–5008.

Goudet, J. 2005. Hierfstat, a package for R to compute and test hierarchical *F*-statistics. *Mol. Ecol. Notes* **5:** 184–186.

Gravem, S. A., W. N. Heady, V. R. Saccomanno, K. F. Alvstad, A. L. M. Gehman, T. N. Frierson, and S. L. Hamilton. 2021. *Pycnopodia helianthoides* (amended version of 2020 assessment). [Online]. The IUCN Red List of Threatened Species 2021: e.T178290276A197818455. Available: https://doi.org/10.2305/IUCN.UK.2021-1.RLTS.T178290276A197818455.en [2022, December 13].

Gurgel, C. F. D., O. Camacho, A. J. Minne, T. Wernberg, and M. A. Coleman. 2020. Marine heatwave drives cryptic loss of genetic diversity in underwater forests. *Curr. Biol.* **30:** 1199–1206.

Gutenkunst, R. N., R. D. Hernandez, S. H. Williamson, and C. D. Bustamante. 2009. Inferring the joint demographic history of multiple populations from multidimensional SNP frequency data. *PLoS Genet.* **5:** e1000695.

Haasl, R. J., and B. A. Payseur. 2011. Multi-locus inference of population structure: a comparison between single nucleotide polymorphisms and microsatellites. *Heredity* **106:** 158–171.

Hare, M. P., L. Nunney, M. K. Schwartz, D. E. Ruzzante, M. Burford, R. S. Waples, K. Ruegg, and F. Palstra. 2011. Understanding and estimating effective population size for practical application in marine species management. *Conserv. Biol.* **25:** 438–449.

Harley, C. D. G., M. S. Pankey, J. P. Wares, R. K. Grosberg, and M. J. Wonham. 2006. Color polymorphism and genetic structure in the sea star *Pisaster ochraceus*. *Biol. Bull.* **211:** 248–262.

Hart, M. W., and P. B. Marko. 2010. Densovirus associated with sea-star wasting disease and mass mortality. *Proc. Natl. Acad. Sci. USA* **111:** 17278–17283.

Hewson, I., J. B. Button, B. M. Gudenkauf, B. Miner, A. L. Newton, J. K. Gaydos, J. Wynne, C. L. Groves, G. Hendler, M. Murray, *et al.* 2014. Densovirus associated with sea-star wasting disease and mass mortality. *Proc. Natl. Acad. Sci. USA* **111:** 17278–17283.

Hill, W. G. 1981. Estimation of effective population size from data on linkage disequilibrium. *Genet. Res.* **38:** 209–216.

IPBES (Intergovernmental Science-Policy Platform on Biodiversity and Ecosystem Services). 2019. *Global Assessment Report on Biodiversity and Ecosystem Services of the Intergovernmental Science-Policy Platform on Biodiversity and Ecosystem Services*, E. S. Brondizio, J. Settele, S. Díaz, and H. T. Ngo, eds. IPBES Secretariat, Bonn, Germany.

IPCC (Intergovernmental Panel on Climate Change). 2021. *Climate Change 2021: The Physical Science Basis. Contribution of Working Group I to the Sixth Assessment Report of the Intergovernmental Panel on Climate Change*, V. Masson-Delmotte, P. Zhai, A. Pirani, S. L. Connors, C. Péan, S. Berger, N. Caud, Y. Chen, L. Goldfarb, M. I. Gomis *et al.*, eds. Cambridge University Press, Cambridge.

Ivanova, N. V., J. R. Dewaard, and P. D. N. Hebert. 2006. An inexpensive, automation-friendly protocol for recovering high-quality DNA. *Mol. Ecol. Notes* **6:** 998–1002.

Jaffe, N., R. Eberl, J. Bucholz, and C. S. Cohen. 2019. Sea star wasting disease demography and etiology in the brooding sea star *Leptasterias* spp. *PLoS One* **14:** e0225248.

Jombart, T., and I. Ahmed. 2011. adegenet 1.3-1: new tools for the analysis of genome-wide SNP data. *Bioinformatics* **27:** 3070–3071.

Jurgens, L. J., L. Rogers-Bennett, P. T. Raimondi, L. M. Schiebelhut, M. N. Dawson, R. K. Grosberg, and B. Gaylord. 2015. Patterns of mass mortality among rocky shore invertebrates across 100 km of northeastern Pacific coastline. *PLoS One* **10:** e0126280.

Keenan, K., P. McGinnity, T. F. Cross, W. W. Crozier, and P. A. Prodöhl. 2013. DiveRsity: an R package for the estimation and exploration of population genetics parameters and their associated errors. *Methods Ecol. Evol.* **4:** 782–788.

Keever, C. C., J. Sunday, J. B. Puritz, J. A. Addison, R. J. Toonen, R. K. Grosberg, and M. W. Hart. 2009. Discordant distribution of populations and genetic variation in a sea star with high dispersal potential. *Evolution* **63:** 3214–3227.

Keller, L. F., K. J. Jeffery, P. Arcese, M. A. Beaumont, W. M. Hochachka, J. N. Smith, and M. W. Bruford. 2001. Immigration and the ephemerality of a natural population bottleneck: evidence from molecular markers. *Proc. R. Soc. B. Biol. Sci.* **268:** 1387–1394.

Lambert, P. 2000. *Sea Stars of British Columbia, Southeast Alaska, and Puget Sound.* UBC Press, British Columbia.

Lessios, H. A. 1988. Mass mortality of *Diadema antillarum* in the Caribbean: What have we learned? *Annu. Rev. Ecol. Syst.* **19:** 371–393.

Marandel, F., G. Charrier, J. B. Lamy, S. Le Cam, P. Lorance, and V. M. Trenkel. 2020. Estimating effective population size using RADseq: effects of SNP selection and sample size. *Ecol. Evol.* **10:** 1929–1937.

Marth, G. T., E. Czabarka, J. Murvai, and S. T. Sherry. 2004. The allele frequency spectrum in genome-wide human variation data reveals signals of differential demographic history in three large world populations. *Genetics* **166:** 351–372.

McCabe, R. M., B. M. Hickey, R. M. Kudela, K. A. Lefebvre, N. G. Adams, B. D. Bill, F. M. Gulland, R. E. Thomson, W. P. Cochlan, and V. L. Trainer. 2016. An unprecedented coastwide toxic algal bloom linked to anomalous ocean conditions. *Geophys. Res. Lett.* **43:** 10366–10376.

McGovern, T. M., C. C. Keever, C. A. Saski, M. W. Hart, and P. B. Marko. 2010. Divergence genetics analysis reveals historical population genetic processes leading to contrasting phylogeographic patterns in co-distributed species. *Mol. Ecol.* **19:** 5043–5060.

McPherson, M. L., D. J. I. Finger, H. F. Houskeeper, T. W. Bell, M. H. Carr, L. Rogers-Bennett, and R. M. Kudela. 2021. Large-scale shift in the structure of a kelp forest ecosystem co-occurs with an epizootic and marine heatwave. *Commun. Biol.* **4:** 298.

Melroy, L. M., and C. S. Cohen. 2021. Temporal and spatial variation in population structure among brooding sea stars in the genus *Leptasterias*. *Ecol. Evol.* **11:** 3313–3331.

Melroy, L. M., R. J. Smith, and C. S. Cohen. 2017. Phylogeography of direct-developing sea stars in the genus *Leptasterias* in relation to San Francisco Bay outflow in central California. *Mar. Biol.* **164:** 152.

Menge, B. A., E. B. Cerny-Chipman, A. Johnson, J. Sullivan, S. Gravem, and F. Chan. 2016. Sea star wasting disease in the keystone predator *Pisaster ochraceus* in Oregon: insights into differential population impacts, recovery, predation rate, and temperature effects from long-term research. *PLoS One* **11:** e0153994.

Miner, C. M., J. L. Burnaford, R. F. Ambrose, L. Antrim, H. Bohlmann, C. A. Blanchette, J. M. Engle, S. C. Fradkin, R. Gaddam, C. D. G. Harley *et al.* 2018. Large-scale impacts of sea star wasting disease (SSWD) on intertidal sea stars and implications for recovery. *PLoS One* **13:** e0192870.

Morin, P. A., K. K. Martien, and B. L. Taylor. 2009. Assessing statistical power of SNPs for population structure and conservation studies. *Mol. Ecol. Resour.* **9:** 66–73.

Nakamura, H., K. Teshima, and H. Tachida. 2018. Effects of cyclic changes in population size on neutral genetic diversity. *Ecol. Evol.* **8:** 9362–9371.

Nei, M. 1987. *Molecular Evolutionary Genetics*. Columbia University Press, New York.

Nunziata, S. O., and D. W. Weisrock. 2017. Estimation of contemporary effective population size and population declines using RAD sequence data. *Heredity* **120:** 196–207.

Oliver, E. C., M. G. Donat, M. T. Burrows, P. J. Moore, D. A. Smale, L. V. Alexander, J. A. Benthuysen, M. Feng, A. S. Gupta, A. J. Hobday *et al.* 2018. Longer and more frequent marine heatwaves over the past century. *Nat. Commun.* **9:** 1–12.

Ortiz, J. C., N. H. Wolff, K. R. Anthony, M. Devlin, S. Lewis, and P. J. Mumby. 2018. Impaired recovery of the Great Barrier Reef under cumulative stress. *Sci. Adv.* **4:** p.eaar6127.

Ovenden, J. R., D. Peel, R. Street, A. J. Courtney, S. D. Hoyle, S. L. Peel, and H. Podlich. 2007. The genetic effective and adult census size of an Australian population of tiger prawns (*Penaeus esculentus*). *Mol. Ecol.* **16:** 127–138.

Overcast, I. 2022. easyFSF. [Online]. Available: https://github.com/isaacovercast/easySFS [2022, December 5].

Padrón, M., F. Costantini, L. Bramanti, K. Guizien, and M. Abbiati. 2018. Genetic connectivity supports recovery of gorgonian populations affected by climate change. *Aquat. Conserv.* **28:** 776–787.

Paine, R. T. 1966. Food web complexity and species diversity. *Am. Nat.* **100:** 65–75.

Palstra, F. P., and D. E. Ruzzante. 2008. Genetic estimates of contemporary effective population size: What can they tell us about the importance of genetic stochasticity for wild population persistence? *Mol. Ecol.* **17:** 3428–3447.

Penn, J. L., and C. Deutsch. 2022. Avoiding ocean mass extinction from climate warming. *Science* **376:** 524–526.

Peterson, B. K., J. N. Weber, E. H. Kay, H. S. Fisher, and H. E. Hoekstra. 2012. Double digest RADseq: an inexpensive method for *de novo* SNP discovery and genotyping in model and non-model species. *PLoS One* **7:** e37135.

Piatt, J. F., J. K. Parrish, H. M. Renner, S. K. Schoen, T. T. Jones, M. L. Arimitsu, K. J. Kuletz, B. Bodenstein, M. García-Reyes, R. S. Duerr *et al.* 2020. Extreme mortality and reproductive failure of common murres resulting from the northeast Pacific marine heatwave of 2014–2016. *PLoS One* **15:** e0226087.

Pilczynska, J., S. Cocito, J. Boavida, E. Serrão, and H. Queiroga. 2016. Genetic diversity and local connectivity in the Mediterranean red gorgonian coral after mass mortality events. *PLoS One* **11:** e0150590.

Pujolar, J. M., S. Vincenzi, L. Zane, D. Jesensek, G. A. De Leo, and A. J. Crivelli. 2011. The effect of recurrent floods on genetic composition of marble trout populations. *PLoS One* **6:** e23822.

Puritz, J. B. 2022. dDocent scripts. [Online]. Available: https://github.com/jpuritz/dDocent/tree/master/scripts [2022, December 5].

Puritz, J. B., and R. J. Toonen. 2011. Coastal pollution limits pelagic larval dispersal. *Nat. Commun.* **2:** 226.

Puritz, J. B., C. C. Keever, J. A. Addison, M. Byrne, M. W. Hart, R. K. Grosberg, and R. J. Toonen. 2012. Extraordinarily rapid life-history divergence between *Cryptasterina* sea star species. *Proc. R. Soc. B Biol. Sci.* **279:** 3914–3922.

Puritz, J. B., C. M. Hollenbeck, and J. R. Gold. 2014. dDocent: a RADseq, variant-calling pipeline designed for population genomics of non-model organisms. *PeerJ* **2:** e431.

Puritz, J. B., J. R. Gold, and D. S. Portnoy. 2016. Fine-scale partitioning of genomic variation among recruits in an exploited fishery: causes and consequences. *Sci. Rep.* **6:** 36095.

Puritz, J. B., C. C. Keever, J. A. Addison, S. S. Barbosa, M. Byrne, M. W. Hart, R. K. Grosberg, and R. J. Toonen. 2017. Life-history predicts past and present population connectivity in two sympatric sea stars. *Ecol. Evol.* **7:** 3916–3930.

R Core Team. 2020. R: a language and environment for statistical computing. [Online]. R Foundation for Statistical Computing, Vienna. Available: http://www.R-project.org [2022, December 5].

Radwan, J., A. Biedrzycka, and W. Babik. 2010. Does reduced MHC diversity decrease viability of vertebrate populations? *Biol. Conserv.* **143:** 537–544.

Rogers-Bennett, L., and C. A. Catton. 2019. Marine heat wave and multiple stressors tip bull kelp forest to sea urchin barrens. *Sci. Rep.* **9:** 1–9.

Rozas, J., A. Ferrer-Mata, J. C. Sánchez-DelBarrio, S. Guirao-Rico, P. Librado, S. E. Ramos-Onsins, and A. Sánchez-Gracia. 2017. DnaSP 6: DNA sequence polymorphism analysis of large data sets. *Mol. Biol. Evol.* **34:** 3299–3302.

Ruiz-Ramos, D. V., L. M. Schiebelhut, K. J. Hoff, J. P. Wares, and M. N Dawson. 2020. An initial comparative genomic autopsy of wasting disease in sea stars. *Mol. Ecol.* **29:** 1087–1102.

Ryman, N., S. Palm, C. Andre, G. R. Carvalho, T. G. Dahlgren, P. E. Jorde, L. Laikre, L. C. Larsson, A. Palme, and D. E. Ruzzante. 2006. Power for detecting genetic divergence: differences between statistical methods and marker loci. *Mol. Ecol.* **15:** 2031–2045.

Schiebelhut, L. M., J. B. Puritz, and M. N Dawson. 2018. Decimation by sea star wasting disease and rapid genetic change in a keystone species, *Pisaster ochraceus*. *Proc. Natl. Acad. Sci. USA* **115:** 7069–7074.

Turner, T. F., J. P. Wares, and J. R. Gold. 2002. Genetic effective size is three orders of magnitude smaller than adult census size in an abundant, estuarine-dependent marine fish (*Sciaenops ocellatus*). *Genetics* **162:** 1329–1339.

Uthicke, S., B. Schaffelke, and M. Byrne. 2009. A boom-bust phylum? Ecological and evolutionary consequences of density variations in echinoderms. *Ecol. Monogr.* **79:** 3–24.

Vázquez-Luis, M., E. Álvarez, A. Barrajon, J. R. Garcia-March, A. Grau, I. E. Hendriks, S. Jiménez, D. Kersting, D. Moreno, M. Perez *et al.* 2017. SOS *Pinna nobilis*: a mass mortality event in western Mediterranean Sea. *Front. Mar. Sci.* **4:** 220.

Vercelloni, J., B. Liquet, E. V. Kennedy, M. González-Rivero, M. J. Caley, E. E. Peterson, M. Puotinen, O. Hoegh-Guldberg, and K. Mengersen. 2020. Forecasting intensifying disturbance effects on coral reefs. *Glob. Change Biol.* **26:** 2785–2797.

Vilas, A., A. Pérez-Figueroa, H. Quesada, and A. Caballero. 2015. Allelic diversity for neutral markers retains a higher adaptive potential for quantitative traits than expected heterozygosity. *Mol. Ecol.* **24:** 4419–4432.

Waples, R. S. 2005. Genetic estimates of contemporary effective population size: To what time periods do the estimates apply? *Mol. Ecol.* **14:** 3335–3352.

Waples, R. S. 2006. A bias correction for estimates of effective population size based on linkage disequilibrium at unlinked gene loci. *Conserv. Genet.* **7:** 167–184.

Waples, R. S. 2016. Making sense of genetic estimates of effective population size. *Mol. Ecol.* **25:** 4689–4691.

Waples, R. S., and C. Do. 2010. Linkage disequilibrium estimates of contemporary N_e using highly variable genetic markers: a largely untapped resource for applied conservation and evolution. *Evol. Appl.* **3:** 244–262.

Wares, J. P., A. R. Hughes, and R. K. Grosberg. 2005. Mechanisms that drive evolutionary change: insights from species introductions and invasions. Pp. 229–257 in *Species Invasions: Insights into Ecology, Evolution, and Biogeography*, D. F. Sax, J. J. Stachowicz, and S. D. Gaines, eds. Sinauer, Sunderland, MA.

Weir, B. S., and C. C. Cockerham. 1984. Estimating *F*-statistics for the analysis of population structure. *Evolution* **38:** 1358–1370.

Wootton, J. T., C. A. Pfister, and J. D. Forester. 2008. Dynamic patterns and ecological impacts of declining ocean pH in a high-resolution multi-year dataset. *Proc. Natl. Acad. Sci. USA* **105:** 18848–18853.